

Effect of nose perturbation on asymmetric vortices over a blunt-nose body at high angle of attack

Sha Y.X.¹, Wang Y.K.² and Qi Z.Y.³

¹ Master Student, Ministry-of-Education Key Laboratory of Fluid Mechanics, Beihang University, Beijing, 100191, China

² Professor, Ministry-of-Education Key Laboratory of Fluid Mechanics, Beihang University, Beijing, 100191, China

³ Ph.D Candidate, Ministry-of-Education Key Laboratory of Fluid Mechanics, Beihang University, Beijing, 100191, China

¹ E-mail: yx_sha@163.com

² E-mail: wangyankui@buaa.edu.cn

Abstract. To improve the maneuverability, the modern missiles of blunt-nose slender body configuration are required to flight at high angle of attack where many research show complex asymmetric vortices flow will develop over the slender body. The effect of artificial perturbation located on the nose of a blunt slender body at high angle of attack ($\alpha=50^\circ$) on asymmetric vortices has been investigated with low speed wind tunnel test. The Reynolds number (Re_D) of the experiment was 1.48×10^5 . The experimental results are shown to be the following: Asymmetric flow over blunt-nose body was extremely sensitive to the machining tolerances of the nose and can be governed by the artificial perturbation; with the circumferential angle of artificial perturbation varied a period, asymmetric vortices present a behavior of single-period.

Keywords: Blunt-nose slender body; high angle of attack; asymmetric vortices; low speed; perturbation

Nomenclature

α	=	Angle of attack (degree)
β	=	Angle of sideslip (degree)
φ	=	Rolling angle of model (degree)
θ	=	Azimuthal angle around model (degree)
γ	=	Circumferential angle of artificial perturbation (degree)
ω	=	Meridian angle of artificial perturbation (degree)
ρ_∞	=	Density of freestream (kg/m^3)
V_∞	=	Velocity of freestream (m/s)
q_∞	=	Dynamic pressure ($q_\infty = \rho_\infty V_\infty^2 / 2$)



- Re_D = Reynolds number based on model diameter
 C_p = Pressure coefficient ($C_p = (P - P_0) / q_\infty$)
 C_y = Sectional side force coefficient
 D = Reference diameter of the slender body (m)
 x/D = Non-dimensional pressure station

1. Introduction

With the development of combat aircraft in performance of mobility and agility, the key to winning in modern air combat often depends on air-to-air missiles (AAM). Air combat simulation results show that ^[1] about 40% of that possibly are close combat. America's most advanced combat aircraft F-22 has a variety of weapons, but each of them has at least two AAM, which fully illustrate the important role of AAM in the future air combat. In order to adapt to the requirement of combination of air, space and land battle ^[2], high maneuverability is not only one of the most significant factor to short-range combat missiles, but also the focus and difficulty in researching which all countries in the world are made unremitting efforts to. Currently, strict performances of infrared guidance ^[3] and requirements of thermal protection are put forward for the close combat AAM. As a result, a typical configuration of blunt-nose and slender body has been selected for this kind of high mobility missiles generally. Furthermore, they usually are required to flight at high angle of attack to improve the maneuverability as much as possible ^[4].

Nevertheless, many research ^[5-20] shows that complex asymmetric vortex flow will develop over the slender body at high angle of attack. Because of the uncertainty and unpredictability of asymmetric vortex flow ^[5-7], the large side force induced by it is also uncertain. Since the flow phenomena of asymmetric vortex over slender body at high angle of attack was discovered ^[8] about half a century, a great number of studies on finding the flow mechanism of the uncertain asymmetric vortex flow and how to control it has been carried out. The research of wind tunnel turbulence ^[9-12], vibration model ^[12-13], and roughness of model processing ^[14-17] indicated that asymmetric vortex is extremely sensitive to the processing roughness near the nose of the model. Since 2002, Deng X.Y. and Wang Y.K. ^[18-19] also have found even the model machining tolerances of the nose can result in different asymmetric flow over two models with same geometry. Since the model machining tolerances were random in fact, it made the research on the asymmetric vortex flow lagged. However, a novel idea was promoted based on the previous studies conducted by Deng X.Y. and Wang Y.K. ^[18-19], in which a small artificial micro-perturbation with diameter 0.2mm located close to the model tip is introduced. It was proved that asymmetric vortices flow over slender pointed-nose body was mainly determined by the artificial micro-perturbation and the asymmetric flow over two models with same geometry was repeatable. On this basis, to the question of how to control the asymmetric vortex so as to control side force, in 2004, Defence Research and Development Canada ^[20] conducted a series of detailed studies on pointed-nose missile flight control using micro-actuated flow effectors by means of wind tunnel experiments and numerical simulations. The results show that the setting of micro-actuated flow effectors could provide considerable side force to the missile flight at high angle of attack, and different side force could be obtained when the micro-actuated flow effectors located in different position.

However, at current, it is not enough for the understanding of asymmetric vortex flow over blunt-nose slender body. For example, if the artificial micro-perturbation could play the same role for

blunt-nose slender body? What the effect of nose artificial perturbation on the asymmetric vortices flow over blunt-nose slender body at high angle of attack? Can the side force induced by this asymmetric flow be utilized to control the missile flight? In order to answer these questions, this paper investigates the effect of nose artificial perturbation on asymmetric flow over a blunt-nose slender body at high angle of attack and make better understanding of it through wind tunnel experiments.

2. Experimental Setup

2.1 Wind Tunnel

The wind-tunnel experiments were performed in the closed-loop, low-speed wind tunnel with a test section $1.5 \times 1.5\text{m}$ at Beihang University. The test section was equipped with a C-strut model support fixed on a rotating platform to adjust the model attitude. It is equipped with a servo motor at the end of the model to change the roll angle ϕ . The maximum freestream velocity of test section is 60m/s and the turbulence level is 0.08% . The Reynolds number for the experiment was $Re_D = 1.48 \times 10^5$ based on diameter of afterbody ($D = 66\text{mm}$).

2.2 Model

The model used, sketched in Figure 1, is a blunt-nose slender body with the overall length of $L = 1060\text{mm}$ and the afterbody diameter of $D = 66\text{mm}$. The fineness ratio of model is $L/D = 16.1$. The radius of blunt nose is $r = 27.2\text{mm}$. Between the nose and cylindrical afterbody, there is a conical part with the apex angle of 18° . The pressure taps are located at 7 stations along the body axis as Figure 1 and each station has 24 equal spaced taps. The wind tunnel test model is shown in Figure 2.

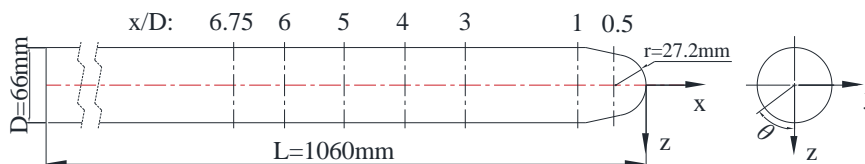


Figure 1. Sketch of test model



Figure 2. Wind tunnel test model

3. Results and Discussion

3.1 Asymmetric vortices flow over blunt-nose slender body at high angle of attack

The side force is usually used to quantify the overall flow asymmetry. In this paper, sectional side

forces (C_y) is calculated by the integral of pressure distribution. Figure 3 shows the sectional side force coefficient changing with roll Angle of model at $\alpha=50^\circ$, $\beta=0^\circ$, $V_\infty=35\text{m/s}$.

As can be seen from Figure 3 (a), the sectional side force coefficient present irregular variation, not only in the magnitude but also the direction, even in the same cross-section ($x/D=3$) since the model is slender body in fact. Figure 3 (b) also shows the sectional side force distributions along slender body model at various roll angles. From the figure the C_y - x/D curves do not coincide with another. Because the side force is induced by asymmetric vortex, it can be seen that asymmetric vortices changing with roll Angle of model present unrepeatable and non-deterministic.

The results from the studies of pointed-nose slender body model [18-19] showed that asymmetric vortex flowfield over slender body was extremely sensitive to the natural disturbances which were produced by geometric imperfect machining tolerances of the nose. As a result, when the model was rolled at a different angle, it would result in a different response of asymmetric vortices as shown in Figure 3.

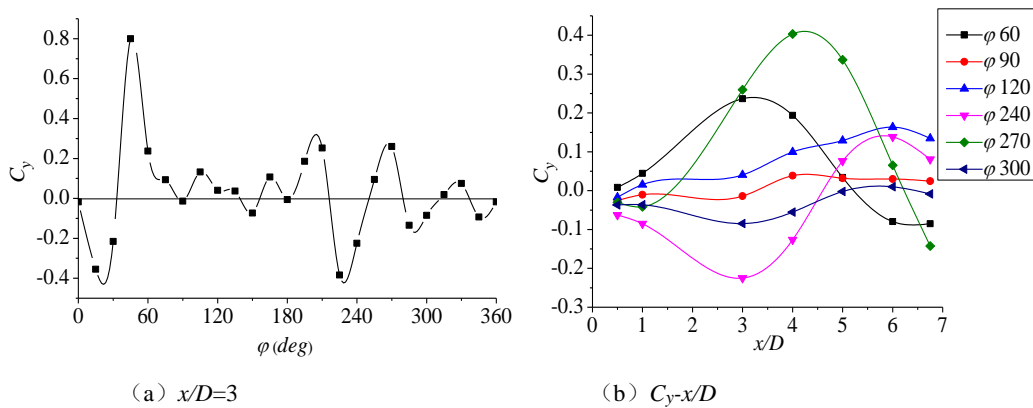


Figure 3. Sectional side force coefficient changing with roll Angle of model ($\alpha=50^\circ$, $\beta=0^\circ$, $V_\infty=35\text{m/s}$)

3.2 Effect of artificial perturbation on the asymmetric vortices flow

In order to investigate the effect of artificial perturbation on the asymmetric vortices flow over blunt-nose slender body model, a small artificial perturbation located on the nose of the model is introduced.

In this paper, a small wood cube with length of $L_p=2\text{mm}$, width of $W_p=1\text{mm}$ and height of $H_p=1\text{mm}$ is selected, which is shown in Figure 4. The location of artificial perturbation is present in Figure 5, in which ω represents the meridian angle and γ is the circumferential angle.



Figure 4. Artificial perturbation model

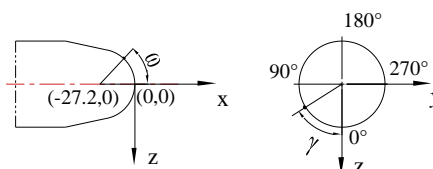


Figure 5. Location of artificial perturbation

Figure 6 presents the characteristic of sectional side force coefficient changing with

circumferential angle of artificial perturbation for the conditions of $\alpha=50^\circ$, $\beta=0^\circ$, $V_\infty=35\text{m/s}$. Compared with Figure 3, it can be proved that the behaviors of asymmetric vortices relate to the location of artificial perturbation, and it means, compare to natural disturbances, the artificial perturbation on the nose of model has the main control to the asymmetric vortices flow. Figure 6 also shows that with the circumferential angle of artificial perturbation varies a period, asymmetric vortices present a behavior of single-period.

Figure 7 and Figure 8 give the pressure distributions of section $x/D=3$ and sectional side force along slender body at 6 different circumferential angle of artificial perturbation, respectively. When the circumferential angle (γ) is between 0° to 180° , the asymmetric vortices flowfield over the model exhibit Left Vortex ^[19] and there is a strong suction peak near leeside of $\theta=165^\circ$. When γ is between 180° to 360° , the asymmetric vortices exhibit Right Vortex ^[19] and the suction peak appear in leeside of $\theta=195^\circ$.

Therefore, it is feasible that the asymmetric vortices flowfield over the blunt-nose slender body can be controlled by adjusting the circumferential location of artificial perturbation on the nose so that a novel side force control technique can be promoted by adjusting artificial perturbation.

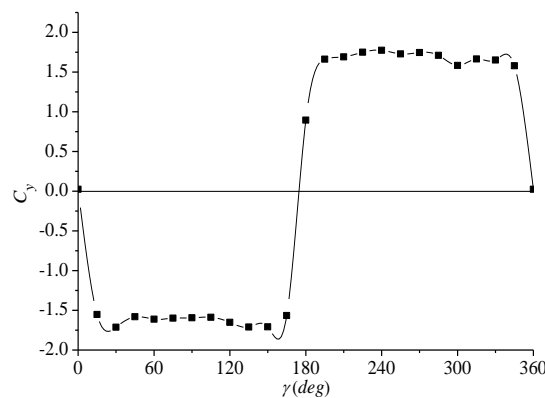


Figure 6. Sectional side force coefficient vs circumferential angle of artificial perturbation ($\alpha=50^\circ$, $\beta=0^\circ$, $V_\infty=35\text{m/s}$, $\omega=40^\circ$, $x/D=3$)

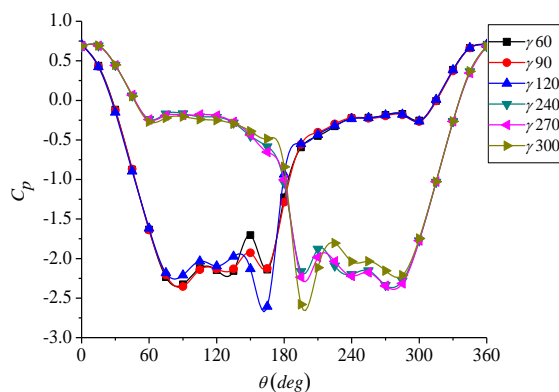


Figure 7. Pressure distributions at various circumferential angle of artificial perturbation ($\alpha=50^\circ$, $\beta=0^\circ$, $V_\infty=35\text{m/s}$, $\omega=40^\circ$, $x/D=3$)

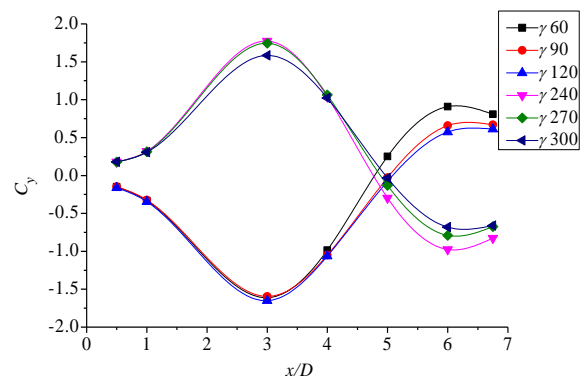


Figure 8. Sectional side force along slender body at various circumferential angle of artificial perturbation ($\alpha=50^\circ$, $\beta=0^\circ$, $V_\infty=35\text{m/s}$, $\omega=40^\circ$)

4. Conclusions

Based the above discussion, the following conclusions can be made:

(1) Asymmetric vortex flowfield over blunt-nose slender body was extremely sensitive to the natural disturbances which were produced by geometric imperfect machining tolerances of the nose.

(2) Compare to natural disturbances, the artificial perturbation on the nose of model has the main control to the asymmetric vortices flow.

(3) With the circumferential angle of artificial perturbation varied a period, asymmetric vortices present a behavior of single-period. As a result, a novel side force control technique can be promoted by adjusting artificial perturbation.

Acknowledgements

The project is supported by the National Natural Science Foundation of China (11472028), the Open fund from State Key Laboratory of Aerodynamics and Shanghai Aerospace Innovation Fund (SAST201443).

References

- [1] Fan H T, Liu D J. Development trends of short-range dogfight IR air to air missile[J]. I. and L. Engineering, 10, 2005
- [2] Zhang B J, Yang X and Ma M. The foreign development of air-to-air missile[J]. China E and Trade H, 73-75, 9, 2014
- [3] Fan H T, Liu D J. The development prospects of close combat about infrared air-to-air missile[J]. I. and L. Engineering, 5, 2005
- [4] Zhu B L. Air-to-air missile and the modern air combat[B]. Air-to-air missile Issue
- [5] Deng X Y, Wang Y K. Asymmetric vortices flow over slender body and its active control at high angle of attack. ACTA Mechanica Sinica, 20(6): 567-579, 2004.
- [6] Chen X R, Deng X Y, Wang Y K. Influence of nose perturbations on behaviors of asymmetric vortices over slender body. ACTA Mechanica Sinica, 18(6): 581-593, 2002.
- [7] Deng X Y, Tian W, Ma B F, et al. Recent progress on the study of asymmetric vortex flow over slender bodies. ACTA Mechanica Sinica, 24(5): 475-487, 2008.
- [8] Allen, H.J. and Perkins, E.W., Characteristics of Flow over Inclined Bodies of Revolution, NACA RM A50L07, 1951.
- [9] Hunt B. L. Asymmetric Vortex Forces and Wakes on Slender Bodies[R]. AIAA-82-1336
- [10] Ericsson L. E. Vortex Unsteadiness on Slender Bodies at High Incidence[J]. J. Aircraft, 1987, V24(4): 319-326
- [11] Dexter P. C. A Study of Asymmetric Flow over Slender Bodies at High Angles of Attack in a Low Turbulence Environment[R]. AIAA-84-0505
- [12] Zilliac G. G., Degani D., Tobak M. Asymmetric Vortices on a Slender Body of Revolution[J]. AIAA Journal, 1991, V29(5): 667-675
- [13] Ericsson L. E., Reding J. P. Aerodynamic Effects of Asymmetric Vortex Shedding from Slender Bodies[R]. AIAA-85-1797
- [14] Levy Y., Hesselink L., Degani D. A Systematic Study of the Correlation Between Geometrical Disturbances and Flow Asymmetries[R]. AIAA-95-0365

- [15] Bridges D. H., Hornung H. G. Elliptic Tip Effects on the Vortex Wake of an Axisymmetric Body at Incidence[J]. AIAA Journal, 1994, V32(7): 1437-1445
- [16] Ward K. C. Boundary Layer Separation and the Vortex Structures around an Inclined Body of Revolution[R]. AIAA-87-2276
- [17] Moskovitz C. Experimental Investigation of a New Device to Control the Asymmetric Flowfield on Forbodies at Large Angles of Attack[R]. AIAA-90-0069
- [18] Deng Xueying, Chen Xuerui, Wang Yankui, et.al., Influence of Nose Perturbations on Behaviors of Asymmetric Vortices over Slender Body, AIAA paper 2002-4710, 2002.
- [19] Deng Xueying, Wang Yankui et.al., Deterministic Flow Field and Flow structure Model of Asymmetric Vortices over Slender Body, AIAA paper 2003-5475, 2003.
- [20] Wong F.C. Missile Flight Control Using Micro-actuated Flow Effectors, Review of fiscal year 2004/2005 progress. DRDC Valcartier TN 2005-282